

REPORT DOCUMENTATION PAGE

AFRL-SR-AR-TR-06-0073

Public reporting burden for this collection of information is estimated to average 1 hour per response, including the time for reviewing instru data needed, and completing and reviewing this collection of information. Send comments regarding this burden estimate or any other asp this burden to Department of Defense, Washington Headquarters Services, Directorate for Information Operations and Reports (0704-0188 4302. Respondents should be aware that notwithstanding any other provision of law, no person shall be subject to any penalty for failing to valid OMB control number. PLEASE DO NOT RETURN YOUR FORM TO THE ABOVE ADDRESS.

1. REPORT DATE (DD-MM-YYYY) 2/28/06		2. REPORT TYPE Final Performance Report		3. DATES COVERED (From - to) 12/1/02 - 11/30/06	
4. TITLE AND SUBTITLE Biomolecular Profiling of Jet Fuel Toxicity Using Proteomics				5a. CONTRACT NUMBER	
				5b. GRANT NUMBER F49620-03-1-0089	
				5c. PROGRAM ELEMENT NUMBER	
6. AUTHOR(S) Frank A. Witzmann, Ph.D.				5d. PROJECT NUMBER	
				5e. TASK NUMBER	
				5f. WORK UNIT NUMBER	
7. PERFORMING ORGANIZATION NAME(S) AND ADDRESS(ES) Department of Cellular & Integrative Physiology Indiana University School of Medicine Biotechnology Research & Training Center 1345 W. 16th St., Room 308 Indianapolis IN 46202				8. PERFORMING ORGANIZATION REPORT NUMBER	
9. SPONSORING / MONITORING AGENCY NAME(S) AND ADDRESS(ES) AFOSR/NL 801 North Randolph Street Room 732 Arlington VA 22203-1977 <i>Dr. Walter Kozumbo</i>				10. SPONSOR/MONITOR'S ACRONYM(S) AFOSR/PK2	
				11. SPONSOR/MONITOR'S REPORT NUMBER(S)	
12. DISTRIBUTION / AVAILABILITY STATEMENT Approval for public release; distribution is unlimited.					
13. SUPPLEMENTARY NOTES <div style="text-align: center; font-size: 2em; font-weight: bold;">20060323058</div>					
14. ABSTRACT This project used a proteomic approach consisting of two-dimensional electrophoresis and mass spectrometry to analyze differential expression in response to JP-8 jet fuel exposure. Protein profiles were generated for whole mouse lung, rat pulmonary alveolar type II cells and macrophages, and human epidermal keratinocytes in various exposure models. Results strongly suggest an injurious effect of exposure on all cells studied. In both pulmonary and skin cells, the protein profiles of JP-8 effect corroborates previous histological findings and point to cytoskeletal alterations as well as impaired secretory and detoxification systems. The addition of substance P to the culture medium prevented the JP-8-mediated loss of an antioxidant protein peroxiredoxin I. Though this was observed only at high-dose JP-8 exposure in vitro, it suggests that substance P may exert it's previously established protection against et fuel injury, by enabling such protein recovery.					
15. SUBJECT TERMS					
16. SECURITY CLASSIFICATION OF:			17. LIMITATION OF ABSTRACT	18. NUMBER OF PAGES	19a. NAME OF RESPONSIBLE PERSON Frank A. Witzmann
a. REPORT UNCLASSIFIED	b. ABSTRACT UNCLASSIFIED	c. THIS PAGE UNCLASSIFIED			19b. TELEPHONE NUMBER (include area code) 317-278-5741

1 Introduction

The overall goal of this project was to analyze protein expression profiles of cells exposed to JP-8 jet fuel using proteomics to better understand the nature of JP-8's toxicity at the molecular (protein) level. Specifically, two-dimensional electrophoresis (2DE) and mass spectrometry were used to separate, detect, quantify, and identify proteins in lung and skin cells whose expression was altered in some way by exposure to JP-8. Samples from JP-8 exposed (*in vivo* and *in vitro*) lungs and pulmonary epithelial cells (in cooperation with the Witten Lab, U. of Ariz.) and human epidermal keratinocytes (in cooperation with the Riviere Lab, NCSU) were obtained and cell lysate proteins studied. With an emerging interest in potential intervention by Substance P (SP) in the pulmonary effects of JP-8 exposure, studies incorporating SP treatment along with JP-8 exposure were also conducted. An additional, emerging goal became the improvement of sensitivity and dynamic range of the analyses, as the limits of the 2DE technique became apparent. Several improvements in the approach to sample preparation were made. These included prefractionation of whole tissue lysates by solution isoelectric focusing, and the addition of a novel reduction/alkylation protocol to improve both the resolution of proteins with alkaline pI as well as the detection of phosphopeptides during tandem mass spectrometry. The results of these experiments are summarized in this report. All figures and tables referred to in the text appear at the end of this document in the Appendix.

2 Methods

2.1 Cell Culture/Animal JP-8 Exposure

2.1.1 Alveolar Type II (AII) and Pulmonary Alveolar Macrophage (PAM) Cells. A transformed rat AII cell line, RLE-6TN was maintained in BRFF-RLuE culture media (BRFF, Ijamsville, MD) containing 10% fetal bovine serum and penicillin/streptomycin antibiotics (pen./strep., Sigma, St. Louis, MO). Cells were cultured in 12-well plates (Fischer Scientific, Pittsburgh, PA) at a density of 10^5 cells/ml. Cell media was replenished every 24–30 h until 95% confluence was achieved and the JP-8 exposures commenced. In all the conditions used in the tests, cell viability, as determined by trypan blue exclusion, was >95% [1].

Primary rat PAMs were isolated from pathogen-free male Fischer 344 rats (Harlan, Indianapolis, IN). The rats were anesthetized intramuscularly with ketamine HCL (80 mg/kg; Parke-Davis, Morris Plains, NJ), xylazine (10 mg/kg; Mobay Corp., Shawnee, KS), and acepromazine maleate (3 mg/kg; Fermenta Animal Health Co., Kansas City, MO). A tracheostomy was performed, with the insertion of a Teflon #18 gauge catheter (Critikon, Tampa Bay, FL) as an endotracheal tube. The rats were killed by exsanguination of the abdominal aorta. The lungs were removed and lavaged with 3 ml aliquots of normal sterile saline warmed to 37°C for a total of six washes. The lavaged total cell numbers and PAM differentials (95–98%) were determined from 0.2-ml sample by hemocytometer counting and cytocentrifuge preparation stained with Diff-Quik (Dade Diagnostics, Aguada, Puerto Rico), respectively. The remaining lavaged fluid was pooled and centrifuged at 400×g for 10 min to obtain a cell pellet. The saline

supernatant was decanted and cells were resuspended in BRFF-RLuE media supplemented with 1× pen./strep. cell culture media. Cells were then counted using a standard hemocytometer and placed in 12-well plates alone at a density of 104 cells/ml. After 1 h of adherence at 37 °C/5% CO₂, cells were washed once with media to remove non-adherent cells and debris and replaced with fresh media. Also, PAM were co-cultured with RLE-6TN cells at a ratio of 4:1, which is the approximate ratio of AIIE cells (14%) to PAM (3%) in the normal rat lung.

JP-8 jet fuel was dissolved in BRFF-RLuE media in 1 µl of 100% ethanol as vehicle and dissolved in media to obtain the appropriate concentrations. Control AIIE and PAM cultures had cell culture media alone or cell culture media with EtOH vehicle. BRFF-RLuE media was removed from cell culture wells and replaced with either control media or JP-8 jet fuel-supplemented media. Cells were then incubated in media for 24 h at which time the media was removed and samples were frozen at -70 °C until cytokine analyzes. Frozen plates (-80°C) with cells adhering were shipped over night on dry ice to Indiana Univ. for 2-DE analysis.

2.1.2 Mouse Lungs. Male Swiss-Webster mice (18-20 g) were randomly assigned into two groups, n=15/group, for either JP-8 jet fuel exposure or controls. Briefly, as in previous studies, JP-8 jet fuel blend (obtained from Wright-Patterson AFB Fuel Laboratory, OH) aerosol was generated using an Ultra-Neb Model #99 nebulizer (DeVilbiss, Somerset, PA). The aerosolized JP-8 vapor was allowed to mix with ambient air after which it was drawn through a 24-port IN-TOX nose-only inhalation chamber using a constant vacuum flow of 0.143 l/min, Total daily exposure time was 1 h repeated for a total of 7 days. This equated to an average JP-8 jet Fuel exposure concentration of 50 mg/m³. JP-8 jet fuel concentrations and particle sizes were determined using a seven-stage cascade impactor (IN-TOX). Control animals were handled in an identical manner to the JP-8 group except that they were exposed to ambient air. The IN-TOX chamber is designed for nose-only exposure to minimize oral ingestion of JP-8 jet fuel during grooming, which more accurately simulated occupational exposures. Euthanasia of the mice occurred on day 7 via CO₂ asphyxiation.

2.1.3 Human Epidermal Keratinocytes. Cryopreserved human neonatal epidermal keratinocytes (HEKs) (approximately 260 K cells/vial) were purchased from Cambrex BioScience (Walkerville, MD) and plated onto three 75-cm² culture flasks, each containing 15 ml of serum-free keratinocyte growth media (KGM-2; from keratinocyte basal media supplemented with 0.1 ng/ml human epidermal growth factor, 5 mg/ml insulin, 0.4% bovine pituitary extract, 0.1% hydrocortisone, 0.1% transferrin, 0.1% epinephrine and 50 mg/ml gentamicin/50 ng/ml amphotericin-B). The culture flasks were maintained in a humidified incubator at 37°C with a 95% O₂/5% CO₂ atmosphere. After reaching approximately 50% confluency, the keratinocytes were passed into eight 75-cm² culture flasks and grown in 15 ml of KGM-2 after which they were harvested and plated in 6-well culture plates in 2 mL of media at a concentration of approximately 96,000 cells per well. Cells were dosed with 0.1% JP-8 (100 µl fuel in 900 µl EtOH stock; 250 µl of stock added to 25 ml pre-warmed KGM-2, mixed well, and dosed 2 ml per well). The cells were exposed to JP-8 for 24 h and cell media collected and frozen

immediately at -80°C for IL-8 determination, in triplicate, using a human IL-8 cytosol (Biosource International, Camarillo CA). Previous studies in our lab have demonstrated ethanol effects on neither protein nor RNA transcription in this model (Allen et al., 2001), therefore no EtOH controls were run. Other plates containing the cells (1 control plate, 2 JP-8 plates, media removed) were quickly frozen at -80°C and shipped overnight for proteomic analysis.

2.2 Sample preparation

2.2.1 Lung tissues.

Samples were frozen at -80°C and shipped from Arizona to Indiana on dry ice, overnight. Tissues were placed in 50 mL beakers at room temperature and 8 volumes (of wet tissue weight) of a lysis buffer containing 9 M urea (BDH Aristar), 4% Igepal CA-630 (Sigma-Aldrich), 1% DTT (Sigma-Aldrich), 1% carrier ampholytes (pH 3-10) (Pharmalyte, Amersham Biosci.) was quickly added onto the still-frozen tissue, and the tissue thoroughly minced with surgical scissors. The minced tissue sample slurry was then placed in a 3 mL DUALL[®] ground-glass tissue grinder and manually homogenized. The resulting homogenate was then manually sonicated with a Fisher Sonic Dismembrator using 3 x 2 sec bursts at instrument setting #3. Sonication was conducted every 15 min for one hour after which time the samples are placed in Beckman polyallomer centrifuge tubes (1/2 x 2 in) and centrifuged at 100,000 x g for 30 min at 22°C using a Beckman TL-100 ultracentrifuge to remove nucleic acid and insoluble materials. The resulting clarified supernatant was then stored at -80°C . Protein concentration was determined by amido black assay conducted in 96-well plates using the Versamax EXT Microplate Reader with Soft Max Pro. Data was recorded and archived on the Witzmann Lab data storage server.

2.2.2 Pulmonary cells (alveolar macrophages, Type II epithelia, & co-culture) and HEK cells. All cultured cells were solubilized directly in-well (in situ) after removal of medium. 400 μL of lysis buffer containing 9 M urea, 4% Igepal CA-630 ([octylphenoxy] polyethoxyethanol), 1% DTT and 2% carrier ampholytes (pH 8–10.5) were added directly to each well. The culture plates were then placed in a 37°C incubator for 1 h with intermittent manual agitation. After 1 h, the entire volume was removed from each well and placed in 2 mL Eppendorf tubes. Each sample was then sonicated with a Fisher Sonic Dismembrator using 3 x 2 s bursts. Sonication was carried out every 15 min for one hour after which the fully solubilized samples were transferred to a cryotube for storage at -80°C until thawed for analysis.

2.3 Two-dimensional electrophoresis.

2.3.1 First-dimension isoelectric focusing. 24 cm IPG strips of broad (3-10) pH ranges were rehydrated with 500 μL of sample and focused using the Protean II IEF cell (Bio-Rad). For optimal separation, the strips were passively rehydrated with the solubilized sample for 24 hours. Subsequently, they were focused for 120,000 volt-hours using the following progression: 150 V - 2 hrs; 300 V - 3 hrs; 1500 V - 2 hrs; 5000 V - 7 hrs, 7000 V - 7 hrs, 8000 V - 5 hours at a constant temperature of 20°C . Each

strip was equilibrated in 6M Urea, 0.375 M Tris pH 8.8, 4% SDS, 20% glycerol, 2% (w/v) DTT followed by an equilibration in 6M Urea, 0.375 M Tris pH 8.8, 4% SDS, 20% glycerol, 2.5% (w/v) iodoacetamide, then placed on a second-dimension DALT slab gel with a gradient of 11-19% acrylamide.

2.3.2 Second-dimension SDS Slab gel electrophoresis. The second-dimension run was conducted at 160 V for 19 hrs in an ISO-DALT electrophoresis chamber. Twenty second dimension gels were run simultaneously in each gel tank to greatly reduce gel-gel variation. Gels were stained using colloidal Coomassie blue (lower detectable limit, 10-20 ng/spot).

2.3.3 Image Analysis. After staining the gels, protein patterns were analyzed and individual proteins identified using either the GS-800 scanner (BioRad) and PDQuest™ image acquisition and analysis software. Gel patterns were analyzed for both protein quantitation and charge modification by generating a reference 2D pattern that serves as a template to which each 2D protein pattern in the match set (conceivably 20-100 gel patterns, e.g. the "object" patterns) was matched. The reference pattern was constructed by using a representative pattern in one of the groups of gels and assigning a number (SSP) to each detected spot. Correspondence of a protein spot in an object pattern to its counterpart in the master was accomplished by associating the spot number (SSP) in the reference pattern to the object spot. The abundance measurements from each pattern were normalized to correct for slight variations in sample loading or overall stain performance using standard procedures within PDQuest.

2.3.4 Statistical Analysis. Raw quantitative data for each protein spot was exported to Excel for statistical analysis and group comparisons using an unpaired, two-tailed Student's t-test.

2.4 Protein identification and characterization

2.4.1 Peptide Mass Fingerprinting. Protein spots from replicate gels were excised manually, and processed automatically using the multifunctional MultiProbe II Station robot (PerkinElmer). In this automated system, the excised protein spots were de-stained, reduced with dithiothreitol, alkylated with iodoacetamide, and tryptically digested using Promega sequence grade, modified trypsin in preparation for matrix-assisted laser desorption ionization mass spectrometry (MALDI-MS) of the resulting peptides. The peptides were then eluted, cleaned-up/desalted and pre-concentrated by micro solid phase extraction using disposable ZipTip® technology and manually spotted on the MALDI-MS sample target along with α -cyano-4-hydroxycinnamic acid matrix. The MALDI target was then analyzed directly by MALDI-MS using the M@LDI™ (Waters) system. This reflectron/time-of-flight instrument enables the automated acquisition of optimized peptide mass spectra, monoisotopic peptide mass fingerprint determination, and subsequent online interrogation of the ProFound™ Peptide Mass Database. ProFound™ calculates the probability that a candidate in a database search is the protein being analyzed. The Z score is calculated when the result of the input mass search is compared against an estimated random match population, and thus

corresponds to the percentile of the search in the random match population. For example, a Z score of 1.65 for a search means that the identified protein is in the 95th percentile and only 5% of random matches would yield a higher Z score than this particular set of masses. This is a more readily understandable way of expressing the robustness of a protein identification obtained by peptide mass fingerprinting.

2.4.2 Tandem Mass Spectrometry (MS/MS). Proteins not identifiable by peptide mass fingerprinting and those in which post-translational modifications (phosphorylation) are likely (based on phosphoprotein staining) were subjected to LC-MS/MS using an LTQ linear ion-trap mass spectrometer (Thermo Electron). Peptide eluents prepared as described above will be separated chromatographically by HPLC prior to nanoelectrospray-ionization and tandem MS. Each full scan mass spectrum was followed by three Data Dependent MS/MS spectra of the most intense peaks. The data was analyzed by Xcalibur software and the proteins will be identified by the BioWorks 3.1 software suite (Thermo Electron).

To analyze the intact phosphoprotein casein, 600 ng of the undigested casein mixture was resolved on an SB RP C18 column (1mm × 150mm, Agilent Technologies, Palo Alto, CA) using a linear 5-50% acetonitrile gradient with 0.1% formic acid over 40min. MS spectra of m/z range of 650-2000 were collected under ESI mode and analyzed using Bioworks v3.2 biomass analysis software. To sequence the phosphopeptides, the casein tryptic digest (1 µg) was separated by LC using the column and mobile phase gradient described above. Mass spectra of the peptides were collected under ESI mode with m/z range of 650-2000 using a modified "triple play" method, which consecutively recorded full MS, data-dependent zoom and data-dependent MS² scan. A tandem MSⁿ⁺¹ scan also was enabled whenever the NL of the mass of a phosphoric acid (98, 49, and 32.7 ± 0.5) was detected at MSⁿ among the "top 3" most intense ions.

Database searching for the peptide sequence and phosphorylation site mapping was conducted using the TurboSEQUENT search of Bioworks, where a static modification of 105 (MW of 4-VP) for cysteine (C), differential modifications of +80, -18 for S and T, and a differential modification of +16 for methionine oxidation were all considered. A high-confidence peptide sequence match was defined as a TurboSEQUENT result with Xcorr value ≥1.5, 2.5, and 3.5 for singly, doubly, and triply charged ions, respectively. The theoretical m/z calculation was conducted using the sequence of mature bovine α-S1, α-S2, and β-casein, considering the number of alkylating molecules on C residues and the number of covalent phosphates. The nomenclature for the tryptic peptides was determined by the position of the tryptic cut relative to the N terminus of the mature protein sequence. For example, T₁ is the 1st peptide from the N terminus generated by tryptic digestion, T₂ is the 2nd peptide from the N terminus generated by tryptic digestion, and T_{1,2} represents the first 2 peptides generated from tryptic digestion with one missed cleavage.

2.5 Reduction/Alkylation Experiments

Fresh human liver was a generous gift from Dr. C. Max Schmidt, (Dept. of Surgery, Indiana University School of Medicine, Cancer Research Institute). The cytosolic

fraction of liver tissue was isolated by differential centrifugation. Liver was homogenized in a buffer containing 0.25 M sucrose and 10 mM Tris-HCl, pH 7.4 and centrifuged at 100,000 x g for 45 min using a Beckman Type 45 Ti Rotor. Protein denaturation, solubilization, and reduction were performed in a portion of the supernate (cytosol) by the addition of urea, CHAPS, and DTT. Carrier ampholyte (pH 3-10) was also added. The final concentrations for these reagents were 9M urea, 4% CHAPS, 65 mM DTT, and 0.5% pH 3-10 ampholyte. Another portion of the supernate was subjected to the same denaturation, solubilization, and reduction process except TCEP was used instead of DTT. The final TCEP concentration was 10 mM. The sample that had been reduced by TCEP was alkylated with 1/20 volumes of 4-VP (400 mM) for 1 h while vortexing. The reaction was quenched by the addition of the same volume of DTT (400 mM) which destroys excess VP. Frozen mouse brain (Harlan Sprague-Dawley, Indianapolis, IN) was minced and homogenized in 8 volumes of solubilization buffer containing 9M urea, 4% CHAPS, 65 mM DTT, and 0.5% pH 3-10 ampholyte. Samples were centrifuged at 100,000 x g for 20 min using a Beckman TL-100 ultracentrifuge to remove nucleic acid and insoluble materials, and the supernate was collected. Similar to the liver cytosolic proteins, reduction and alkylation with TCEP and VP were carried out for a portion of the brain protein lysate using the same solubilization buffer, but TCEP (10mM) was used instead of DTT. Some of the alkylated and unalkylated sample was pre-fractionated by microscale solution isoelectrofocusing using the Zoom[®] IEF fractionator (Invitrogen, Carlsbad, CA). The protein fractions (alkylated and unalkylated) that were enriched in basic proteins (pI=7-10) were subjected to subsequent IEF on IPGs. In some experimental stages, a protein assay was performed using the RC DC Protein Assay kit (Bio-Rad, Richmond, CA) according to the manufacturer's protocol to determine protein concentration.

First-dimension IEF was performed on IPG strips (pH 3-10, 24cm, Bio-Rad, Richmond, CA). The protein lysate was diluted with rehydration buffer (8 M urea, 2%CHAPS, 15mM DTT, 0.2% ampholytes/pH3-10). Rehydration of IPG strips was carried out overnight at room temperature. The proteins were focused at $\leq 50 \mu\text{A}/\text{strip}$ at 20°C, using progressively increasing voltage up to 10,000 V for a total of 100,000 Vh. Two 10-minute equilibration steps were carried out in equilibration buffer I (6 M urea, 0.375 M Tris, pH 8.8, 2% SDS, 20% glycerol, 2% DTT) equilibration buffer II (6 M urea, 0.375 M Tris, pH 8.8, 2% SDS, 20% glycerol, 2.5% iodoacetamide) respectively for the samples went through the conventional DTT reduction right before the IPG strips were loaded on to the slab gels. A 20 min equilibration step was carried out after IEF for those samples that had been treated with TCEP and VP using equilibration buffer III containing 6 M Urea, 0.375 M Tris, pH 8.8, 2% SDS, and 20% glycerol. Second dimension separation was accomplished on linear 11-19% acrylamide gradient slab gels (20 cm x 25 cm x 1.5 mm), poured and cast reproducibly using a computer-controlled gradient maker. Gels were run simultaneously for approximately 18 h at 160 V and 8°C. Slab gels were stained using a colloidal Coomassie Brilliant Blue G-250 procedure.

3 Results & Discussion

3.1 JP-8 effects on pulmonary cells *in vivo*

Previous collaborative studies have analyzed the effect of high level JP-8 exposure (250, 1000, and 2500 mg/m³) [2-4]. Significant quantitative differences in lung protein expression were found as a result of JP-8 exposure. At 250 mg/m³ JP-8 concentration, 31 proteins exhibited increased expression, while 10 showed decreased expression. At 1000 mg/m³ exposure levels, 21 lung proteins exhibited increased expression and 99 demonstrated decreased expression. At 2500 mg/m³, 30 exhibited increased expression, while 135 showed decreased expression. Several of the proteins were identified by peptide mass fingerprinting, and were found to relate to cell structure, cell proliferation, protein repair, and apoptosis. These data demonstrated the significant stress JP-8 jet fuel puts on lung epithelium. Furthermore, there was a decrease in α 1-antitrypsin expression suggesting that JP-8 jet fuel exposure may have implications for the development of pulmonary disorders.

To evaluate a lower, more occupationally relevant JP-8 exposure, the effect of aerosolized JP-8 exposure at 50 mg/m³ was studied. In the mouse lung, 1,501 protein spots analyzed and an average of 988 were matched across all gels in the experiment (n=5). Of the 42 proteins were identified by PMF, 9 proteins were differentially expressed (P < .005); 3 were decreased and 6 increased in abundance. The down-regulated proteins were primarily of a group involved in the cytoskeleton: **peripherin** (an intermediate filament protein of the multigene family containing vimentin, desmin, glial fibrillary acidic protein, peripherin, and plasticin); **vimentin**; **desmin**; **α tropomyosin**, and **hsp27** (which modulates vimentin filaments). One non-cytoskeletal protein was also downregulated, **cAMP-dependent PK type I-beta regulatory chain** while upregulated proteins were related to a generalized stress response, e.g. **hsp60**.

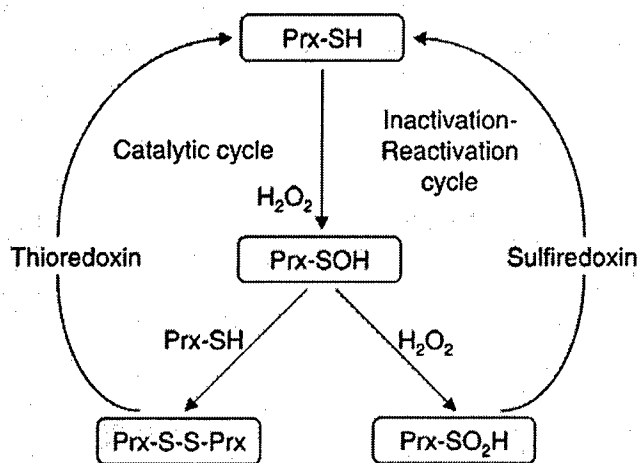
These results suggest a moderate yet significant effect of JP-8 exposure, even at 50 mg/m³, involving differential protein expression consistent with structural alterations observed at higher exposures.

3.2 JP-8 effects on pulmonary cells *in vitro*

Witten et al. has demonstrated *in vivo* that JP-8 inhalation induces a neurogenic inflammatory response in the lungs (JP-8 Meeting, Tucson 2005). However, the mechanisms underlying this effect remains unclear. In those studies, histopathological examination revealed that both pulmonary alveolar macrophages (PAM) and alveolar type II epithelial cells (AIE) are direct targets of JP-8 inhalation. Subsequent *in vitro* studies demonstrated that there seems to be cell-cell communication between co-cultured PAM and AIE exposed to JP-8 jet fuel. Following those studies the relevance of the substance P signal mechanism in the JP-8 jet fuel-mediated proinflammatory response was examined in a co-cultured PAM and AIE cell model. That study documented that the proinflammatory cytokines IL-1 α , IL-1 β levels were elevated in PAM and the co-culture system by a 24 h exposure to JP-8, a response that likely initiates the inflammatory response. JP-8 jet fuel incubation also increased nitric oxide level in type II epithelial cells, but not in macrophages. Substance P or its agonist [Sar9 Met (O2)11] Substance P significantly block this mediator release through obvious different mechanisms including receptor- and non-receptor mediated signal transduction. The cell co-culture data indicated that the balance of these mediators could be regulated possibly by cross communication of both alveolar cells, which reside

in close proximity to each other. These results have not yet been published but were reported at the annual JP-8 meeting in Tucson, in December 2005.

In the current study, we sought to assess JP-8 effects from samples generated by the studies mentioned in the previous paragraph. Our results from 8 $\mu\text{g}/\text{mL}$ JP-8 exposures *in vitro* demonstrated that Sar9, Met (O₂)11-substance P treatment appears to “protect” proteins that have anti-oxidant functions against JP-8 jet fuel exposure in lung cell cultures of pulmonary alveolar macrophages and alveolar epithelial type II cells analyzed by proteomics (Figure 2). Notably, Peroxiredoxin-1 (thioredoxin peroxidase) (see illustration below) levels were vastly decreased due to JP-8 jet fuel exposure, however, Sar9, Met (O₂)11-substance P treatment maintained peroxiredoxin-1 levels



Catalytic and inactivation/activation cycles of 2-Cys Prx enzymes.

after JP-8 jet fuel exposure in the lung cell cultures.

In addition, of 23 proteins altered by JP-8 exposure in the AEII-PAM co-culture system (see Figure 1 in Appendix), 15 were observed to recover significantly with SP treatment. The functions of these proteins were clustered using Gene Ontology database mining, and this result appears in Figure 3.

3.3 JP-8 effects on skin cells *in vitro*

In vivo exposure to JP-8 and other kerosene-based fuels causes skin irritation, skin sensitization and skin tumors with repeated or prolonged contact. Significant immunosuppression has been observed when JP-8 is applied dermally in mice. Overall, JP-8's systemic effects resulting from dermal exposure seem to be minimal, but they have not been studied extensively.

Jet fuel exposure in various types of cultured cells is associated with biological effects that include cytotoxicity, cytokine release, DNA damage, and oxidative stress, indicating the toxic and pro-inflammatory nature of JP-8 and its components [5-8]. In human epidermal keratinocytes (HEK), 0.1% JP-8 in the culture medium has been shown to cause an inflammatory response [9] as have individual neat aliphatic hydrocarbons similarly exposed to HEK [5,6]. *In vitro* exposure to JP-8 also has been shown to alter the expression of members of the Bcl-2 family of proteins that play a major role in both apoptosis and necrosis. JP-8 was shown to upregulate antisurvival members (Bad and Bak) and downregulate prosurvival proteins (Bcl-2 and Bcl-x1), resulting in necrotic rather than apoptotic keratinocyte cell death [10]. In an effort to characterize HEK responses to low level JP-8 exposure (0.01%), Espinoza et al. [11] analyzed gene HEK expression via microarray. As expected, this noninflammatory

exposure failed to upregulate genes for IL-1, IL-8, IL-10, COX-2, and iNOS. However, the expression of a number of discriminant genes was altered, including those involved in stress response, intermediary metabolism, detoxification, and cell growth regulation.

Bearing in mind the often observed discordance between gene expression (when analyzed as quantitative alterations in mRNA) and quantitative alterations in protein expression, we sought to investigate the effect of JP-8 exposure on protein expression, *in vitro*, at an exposure known to cause an inflammatory response. Thus, the primary objective of this portion of the research period was to analyze the effect of JP-8 jet fuel exposure on quantitative and qualitative protein expression in human keratinocytes using an *in vitro* exposure paradigm and a 2-D gel-based proteomic approach. Understanding JP-8's mechanism of action in the germinal epidermis may help in the design of prophylactic or therapeutic intervention to dermal jet fuel exposures.

Consistent with previous *in vitro* exposures to JP-8 or its constituents, 24 h exposure of HEK to 0.1% JP-8 resulted in a significant increase in IL-8 production and release as shown in Figure 4. JP-8 exposure significantly altered the expression of 35 proteins ($P < .02$), of which 33 were identified by peptide mass fingerprinting. These identified proteins and pertinent information regarding their expression are listed in Table 1.

The altered expression of 33 identified proteins after 24 h of exposure suggests that the inflammation also documented here is associated with a limited group of functional changes indicated by the constituent proteins altered (Figure 5). If one assumes that this response occurs *in vivo*, dermal JP-8 exposure creates the potential for chronic inflammation which, in turn, may contribute to the development or progression of disease states in the skin.

As is frequently the case in discovery-based toxicologic investigations such as this, a number of proteins are identified and their expression is altered by the treatment, yet the impact of these changes on the keratinocyte, specifically, and the skin more generally is elusive. To better understand the meaning of the altered proteins and to assess their toxicologic relevance, we have grouped these proteins according to function:

- 1) **Proteins involved in protein synthesis, folding, degradation, and in mRNA processing, transport, and translation.** Upregulated proteins included 26S proteasome non-ATPase regulatory subunit 9, cullin 4B, cyclophilin. Downregulated proteins included the T-complex protein 1, delta subunit; heterogeneous nuclear ribonucleoprotein (hnRNP C), and eukaryotic translation elongation factor 2 (eEF-2).
- 2) **Cytoskeletal proteins and intermediate filaments (cell junction, motility).** In general, we observed the down-regulation of type II keratins and upregulation of type I keratins. Keratins 5, 6, 7 and 8, were both prominently down-regulated. Two type I keratins, 10 and 14, were elevated. Phosphoglucomutase-related protein 5 (PGMRP5) and EphB4 (receptor protein tyrosine kinase variant EphB4v1) were downregulated.
- 3) **Proteins involved in membrane trafficking.** Several related proteins involved at various levels with vesicular processing were all down-regulated by JP-8.

These included ADP-ribosylation factor (ARF) GTPase-activating protein, Rab6 GTPase activating protein (the protein most significantly effected by JP-8), rab6-interacting protein 2, syntaxin-3, flotillin-1, annexin A3, and cappuccino protein homolog. Two additional proteins in this general class were up-regulated by JP-8 exposure, formin-binding protein 17 (FBP17) and Jaw1 (inositol 1,4,5-triphosphate-associated cGMP kinase substrate).

- 4) **Proteins involved in inflammation, injury, and other processes.** In addition to the release of IL-8 by HEK, JP-8 also resulted in the decreased cellular expression of the acute-phase reactant serum amyloid A protein beta (SAA), a protein typically up-regulated by a variety of inflammatory stimuli. Although SAA's decrease seems paradoxical, it may be that its rapid induction and secretion render its intracellular stores (detected by 2-DE) slightly lower than in the untreated control. Upregulated proteins include low-density lipoprotein receptor-related protein 12 (LRP), hsp27, Urf-ret protein (unassigned open reading-frame protein-tyrosine kinase) (cadherin superfamily member), and stress-activated map kinase interacting protein 1 (SAPK interacting protein 1, *aka* Ras inhibitor JC310).

Many of the changes seen in response to JP-8 exposure may actually be a result of specific hydrocarbon fractions, a phenomenon seen under in vitro conditions similar to those employed here, and recently confirmed after in vivo exposure [12]. It is possible that some of the "conflicting" protein changes seen in the present study may be secondary to the complex composition of JP-8 where in reality multiple toxicological changes are occurring secondary to the different fuel components. The linkage of specific components to specific patterns of protein expression deserves further attention.

3.4 Technical Developments – Sample Prefractionation, Reduction and Alkylation for Improved Protein Separation, Dynamic Range and Mass Spectrometry

3.4.1 Sample fractionation by solution isoelectric focusing. With the ability to run literally hundreds of gels with acceptable consistency, 2DE analysis in toxicoproteomics is poised to take advantage of another trend in proteomics, the reduction of sample complexity. It is clear that global protein analysis across the range of protein expression is currently impossible, no matter which proteomics platform one applies. Consequently, the strategy of examining subsets of the proteome has gained significant momentum, and methods to reduce sample complexity in all manner of proteomic studies are becoming routine. In reducing sample complexity, the aim is to accomplish two things: 1) to reduce sample heterogeneity, e.g. rather than using whole liver, kidney or brain homogenate, one uses carefully dissected regions or cells isolated by collagenase treatment and centrifugation or via laser capture, or 2) to improve the analytical "depth of field" by digging deeper into the proteome through the analysis of cell organelles, specific membrane fractions, or multiple sub-proteomes. One can also study specifically enriched proteomic subsets generated by a) depletion of a few highly

S-R2, when R1=R2, represents intra-molecular disulfides) following the oxidation of the cysteinyl thiol groups (-SH). This is primarily due to the depletion of the reducing agent, such as dithiothreitol (DTT) or its isomer dithioerythritol (DTE) in the basic pH range during the first dimension isoelectric focusing (IEF). DTT and DTE contained in the lysis and rehydration buffers are weak acids (pK=8-9), that migrate toward the anode during IEF, leading to the loss of the reducing agent from the basic portion of the IPG strip. In an environment lacking a reducing agent, the cysteinyl thiol groups tend to crosslink again, leading to the restoration of the disulfide bridges.

Optimal IEF in the alkaline region remains a challenge, although various attempts have been made to reduce the streaks. Our novel approach is to prepare samples in a way to prevent the regeneration of the cross-links between cysteinyl thiols by a permanent modification of the free thiol groups through alkylation. This modification is commonly accomplished through a reduction and alkylation process using DTT to reduce the disulfide bonds to free thiol groups and iodoacetamide or non-charged acrylamide derivatives (such as N,N-dimethylacrylamide, DMA) to alkylate free thiols. Unfortunately both iodoacetamide and acrylamide can change the gel patterns or generate extra artifactual spots in 2-DE maps, and streaks cannot be completely eliminated because of incomplete alkylation of the cysteinyl thiols. In fact, both iodoacetamide and non-charged acrylamide derivatives alkylate only 80% of all the thiol groups in the protein.

The formation of intra- and inter-molecular disulfides between these residual thiol groups is still significant to the development of protein aggregation during IEF. The primary reason for an incomplete alkylation is the excess amount of DTT (~20-fold molar excess) that is needed to achieve a complete reduction. When an alkylating agent is added to the reaction, the remaining DTT in the sample will compete with the cysteinyl thiols to react with the alkylating agent, driving the reaction toward the regeneration of disulfide cross links. Trialkylphosphines such as tributylphosphine (TBP) and tris(2-carboxyethyl)-phosphine hydrochloride (TCEP) are powerful reducing agents, which can readily and stoichiometrically reduce disulfides with high specificity. Unlike DTT, trialkylphosphines do not react with some alkylating reagents. It has been shown that TBP greatly improves the protein solubility when used prior to 2-DE. Due to such issues as solubility, odor, and toxicity, reduction with TCEP is more favorable than TBP.

Vinylpyridine (VP) is one of the commonly used protein alkylating agents for the protein digests prior peptide mapping and sequence analysis using mass spectrometry. It has been shown to react with the cysteinyl thiols with 100% specificity and the alkylation is 100% complete. Sebastiano and co-workers compared several alkylating agents, including acrylamide, DMA, iodoacetic acid, 2-vinylpyridine (2-VP), and 4-vinylpyridine (4-VP), and found that VP was the only compound achieved 100% alkylation [13]. We therefore developed a novel reduction and alkylation approach to prepare protein samples for 2-DE to achieve the goal of reducing basic pH end streaks, hence improving the resolution of 2-DE.

Alkylation with VP effectively eliminated the streaks in the basic pH range in 2-DE maps [14]. This "de-streaking" method was efficient in various sample types, including total tissue lysate and protein lysates that had been pre-fractionated (a subcellular fraction or a Zoom[®] IEF fraction). The absence of streaks in the cytosolic protein fraction was not surprising, because "streaky proteins", often membrane proteins, are

associated with such cellular organelles as endoplasmic reticulum (microsomes) and mitochondria. The remarkable efficiency of VP alkylation in streak reduction was further demonstrated in more complex samples, which either contained membrane protein or was enriched in basic proteins. The streaks shown in alkaline region of the 2-DE map for the mouse brain protein lysate were fully eliminated in the corresponding sample that had undergone VP alkylation. Furthermore, the basic protein enriched fraction (pI=7-10) from Zoom[®]IEF, which was shown as the protein streaks in unalkylated sample, was completely resolved in the 2-DE map of the same sample that had been alkylated with VP.

This reduction and alkylation process using TCEP and VP during 2-DE sample preparation has greatly improved resolution in various sample types, particularly for proteins in the basic pH range (e.g. with alkaline pI). These improvements will enhance the analysis and identification of those proteins undergoing quantitative (up/down regulation, presence, absence, etc.) or qualitative (post-translational modification) changes that were previously unanalyzable due to their poor resolution. The improvement in resolution will also allow loading more concentrated samples, thereby enhancing the intensity of the faint protein spots and increasing the number of proteins that can be identified by peptide mass fingerprinting. The technique is suitable for kit development and a provisional patent application has been processed.

With respect to our efforts regarding TCEP/VP applications in phosphoprotein detection using tandem mass spectrometry, this rather lengthy account has been submitted for publication, was recently presented as a poster presentation at the Association for Biomolecular Resource facilities annual meeting in Long Beach CA, and a patent application submitted. The following summarizes this important technical development that we hope to apply to future AFOSR-related toxicoproteomics studies.

The most direct and convincing evidence of the presence of peptide phosphorylation is the observation of characteristic neutral loss of a phosphoric acid under low-energy collision-induced dissociation, reinforced by high-confidence mass spectrometric sequencing. However, the lability of phosphate esters and the low abundance of phosphoproteins create significant challenges to the application of this technique. We have applied a one-step reduction and alkylation treatment using tris(2-carboxyethyl)-phosphine hydrochloride and 4-vinylpyridine to favor the preservation of the phosphate moieties on a protein. Using sequential full MS, data-dependent zoom and MS/MS scans coupled with neutral loss-dependent tandem MSⁿ, a total of 26 phosphorylation sites were identified with high confidence in a rather low quantity (ng-level) casein mixture containing α -S1, α -S2, and β caseins. Two of these sites are novel phosphorylation sites, not having been documented previously. Multilevel confirmations add confidence to the mapping of these phosphorylation events. This technological development can be viewed as an enabling technology, one that may assist proteomics researchers in their important quest to characterize this most-important protein posttranslational modification. We hope to apply this sample preparation method to the analysis of chemical exposure-related alterations in the phosphorylation of proteins, predominant in signaling pathways.

4 Conclusion and Summary

The present results suggest that JP-8 exposure is associated with significant molecular effects, at the protein level, in both animal model pulmonary exposures and in cell cultures using both rodent and human cells. Minor but significant effects observed at 50 mg/m³ suggest that similar analyses at even lower and more acute exposures should be undertaken. High-dose exposures of JP-8 in vitro result in moderate yet significant alterations in alveolar and pulmonary cells in co-culture, primarily in proteins, associated with transport, cell growth and/or maintenance, development, and cellular responses to stimuli.

By way of extrapolation, it is likely that JP-8 jet fuel-induced lung injury presents a health risk to civilian and military personnel through incidental or occupational exposure and that substance P may serve as an effective in ameliorating such effects. Certainly this remains to be confirmed and the utility of other protective agents should be considered and evaluated.

5 References

1. Wang S, Young RS, Sun NN, Witten ML: **In vitro cytokine release from rat type II pneumocytes and alveolar macrophages following exposure to JP-8 jet fuel in co-culture.** *Toxicology* 2002, **173**:211-219.
2. Witzmann FA, Bauer MD, Fieno AM, Grant RA, Keough TW, Kornguth SE, Lacey MP, Siegel FL, Sun Y, Wright LS, et al.: **Proteomic analysis of simulated occupational jet fuel exposure in the lung.** *Electrophoresis* 1999, **20**:3659-3669.
3. Witzmann FA, Bauer MD, Fieno AM, Grant RA, Keough TW, Lacey MP, Sun Y, Witten ML, Young RS: **Proteomic analysis of the renal effects of simulated occupational jet fuel exposure.** *Electrophoresis* 2000, **21**:976-984.
4. Drake MG, Witzmann FA, Hyde J, Witten ML: **JP-8 jet fuel exposure alters protein expression in the lung.** *Toxicology* 2003, **191**:199-210.
5. Chou CC, Riviere JE, Monteiro-Riviere NA: **The cytotoxicity of jet fuel aromatic hydrocarbons and dose-related interleukin-8 release from human epidermal keratinocytes.** *Arch Toxicol* 2003, **77**:384-391.
6. Chou CC, Riviere JE, Monteiro-Riviere NA: **Differential relationship between the carbon chain length of jet fuel aliphatic hydrocarbons and their ability to induce cytotoxicity vs. interleukin-8 release in human epidermal keratinocytes.** *Toxicol Sci* 2002, **69**:226-233.
7. Boulares AH, Contreras FJ, Espinoza LA, Smulson ME: **Roles of Oxidative Stress and Glutathione Depletion in JP-8 Jet Fuel-Induced Apoptosis in Rat Lung Epithelial Cells.** *Toxicol Appl Pharmacol* 2002, **180**:92-99.
8. Monteiro-Riviere N, Inman A, Riviere J: **Effects of short-term high-dose and low-dose dermal exposure to Jet A, JP-8 and JP-8 + 100 jet fuels.** *J Appl Toxicol* 2001, **21**:485-494.
9. Monteiro-Riviere NA, Inman AO, Riviere JE: **Skin toxicity of jet fuels: ultrastructural studies and the effects of substance P.** *Toxicol Appl Pharmacol* 2004, **195**:339-347.

10. Rosenthal DS, Simbulan-Rosenthal CM, Liu WF, Stoica BA, Smulson ME: **Mechanisms of JP-8 jet fuel cell toxicity. II. Induction of necrosis in skin fibroblasts and keratinocytes and modulation of levels of Bcl-2 family members.** *Toxicol Appl Pharmacol* 2001, **171**:107-116.
11. Espinoza LA, Li P, Lee RY, Wang Y, Boulares AH, Clarke R, Smulson ME: **Evaluation of gene expression profile of keratinocytes in response to JP-8 jet fuel.** *Toxicol Appl Pharmacol* 2004, **200**:93-102.
12. Muhammad F, Monteiro-Riviere NA, Riviere JE: **Comparative in vivo toxicity of topical JP-8 jet fuel and its individual hydrocarbon components: Identification of tridecane and tetradecane as key constituents responsible for dermal irritation.** *Toxicologic Pathology* 2005, **33**:258-266.
13. Sebastiano R, Citterio A, Lapadula M, Righetti PG: **A new deuterated alkylating agent for quantitative proteomics.** *Rapid Commun Mass Spectrom* 2003, **17**:2380-2386.
14. Bai F, Liu S, Witzmann FA: **A "de-streaking" method for two-dimensional electrophoresis using the reducing agent tris(2-carboxyethyl)-phosphine hydrochloride and alkylating agent vinylpyridine.** *Proteomics* 2005, **5**:2043-2047.

APPENDIX

Figure 1. Proteins alterations in AEII/PAM co-culture exposed to JP-8 and/or Sar9, Met (O₂)11-substance P

Proteins analyzed 1,355
 Vehicle vs. JP8 (p<.01) 23
 Of those 23, recovery at any SP exposure? 15 (usually 1 μM most effective)

 Proteins ↓ @ 100 μM SP when JP8 is added 28 Vehicle vs. 100 μM SP 14
 Proteins ↓ @ 10 μM SP when JP8 is added 10 Vehicle vs. 10 μM SP 28
 Proteins ↓ @ 1 μM SP when JP8 is added 9 Vehicle vs. 1 μM SP 12

Spot #	Name	Accession	JP8	SP+JP8
2603	COP9 signalosome complex subunit 2)	P61203	■	NE
204	similar to COP9 complex subunit 6 (regulatory, (Ub)/26S proteasome system)	O88545	■	▣
608	SH3P7r4 (Drebrin-like protein) – actin-cytoskeleton regulation	Q9JHL4	■	NE
1320	SNAP-29 protein (Gs32 protein) Golgi snare	Q9Z2P6	■	■
2604	fructose-biphosphatase	P19112	■	NE
226	non-muscle alpha tropomyosin	P04692	■	NE
2621	Ras-GTPase-activating protein binding protein 2	P97379	■	■
1621	syndapin IIab (synaptic dynamin-associated protein II)	Q9QY17	■	■
9022	endothelin-B receptor	Q9R1M2	■	■
503	tropomyosin alpha isoform	Q923Z2	■	▣
5844	nepriylsin II (Enkephalinase) - Metalloprotease	P07861	■	■
1629	Alpha-intermexin	P23565	■	■
9215	Peroxiredoxin 1	Q63716	■	■
8124	glycogen phosphorylase	P09812	■	■
9218	Peroxiredoxin 1	Q63716	■	■
8331	outer mitochondrial membrane protein porin 1; plasmalemmal porin	Q60932	■	■
1632	cytokeratin 14	Q61FV1	■	■
514	SKAP55 adaptor protein	Q8CHI6	■	NE

Figure 2. Clustering by function, those proteins appearing in Figure 1.

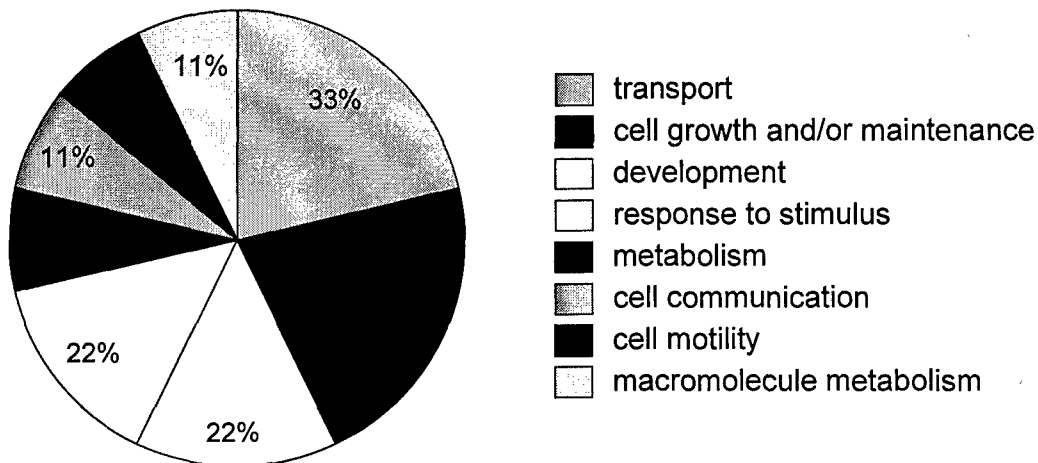


Figure 3. SP protects against the JP8-mediated loss of peroxiredoxin-1 (spot # 9215 and 9218)

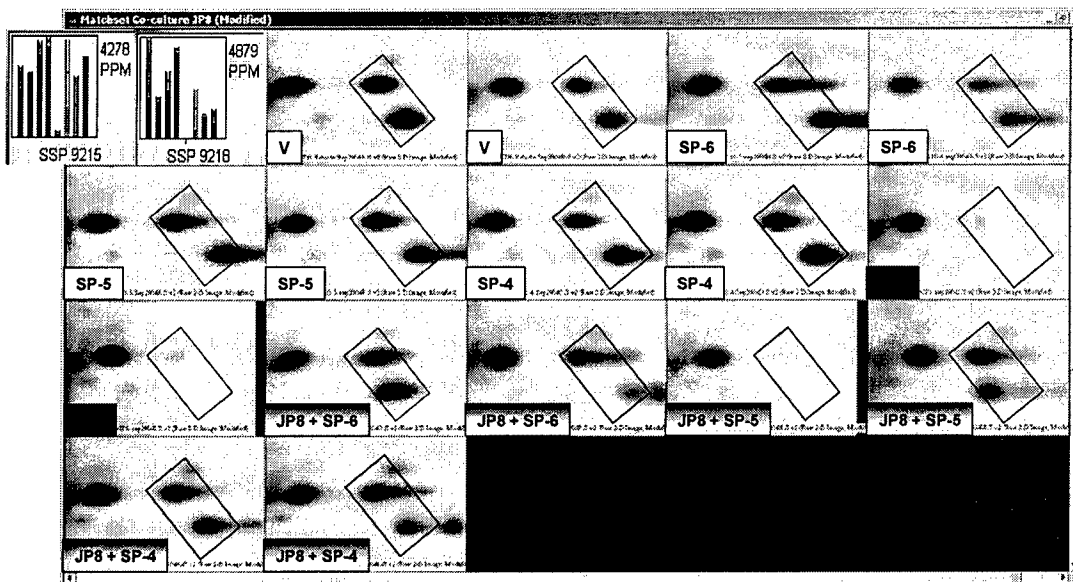


Figure 4.

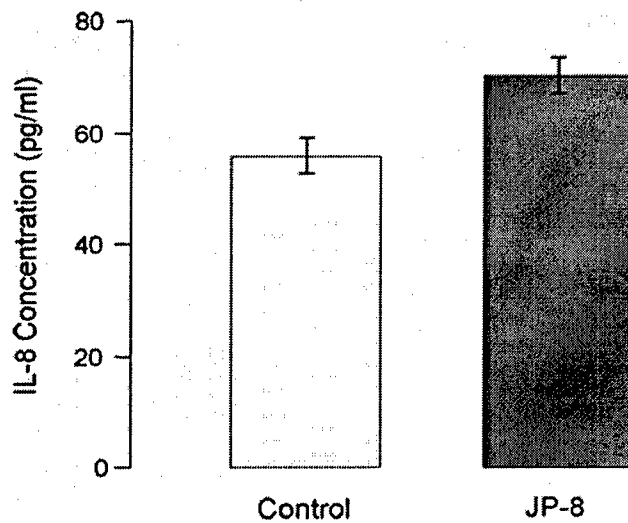


Table 1.

Table 1 Human keratinocyte proteins altered by JP-8 jet fuel exposure and subjected to peptide mass fingerprint identification												
SSP ^a	SwissProt accession	SwissProt entry	Protein name	Control	JP8	Prob ^b	Fold	% Change	Z-score ^c	% Coverage ^d	pI ^e	MW ^e
6003	Q75099	Q75099_human	tab6 GTPase activating protein	1035	402	0.000000001	2.6	-61.2	2.43	31	6.2	16.7
3501	P04729	K2C7_human	Keratin 7, type II	274	172	0.000001	1.6	-37.1	2.43	15	5.4	51.4
1212	Q13277	STX3_human	Syntaxin-3	565	319	0.000004	1.8	-43.5	1.33	27	5.2	31.9
7605	Q96L55	Q96L55_human	EphB4: receptor protein tyrosine kinase variant 1	369	209	0.00001	1.8	-43.4	2.43	10	6.7	104.1
7712	P02747	TRFE_human	Transferrin: D6: beta-1-metal binding globulin	1129	820	0.00001	1.4	-27.4	1.72	13	6.9	79.3
7101	NA	NA	Unknown	323	135	0.00001	2.4	-58.1				
6702	NA	NA	Unknown	327	433	0.0002	1.3	32.3				
8301	Q96LH5	Q96LH5	Fermin-binding protein 17 (FBP17, FLJ113619, FLJ110754, FLJ110113, KIAA0554)	712	869	0.0005	1.2	22.0	2.43	14	8.8	41.1
7806	P13639	EP2_human	Eukaryotic translation elongation factor 2	1696	1032	0.001	1.6	-39.2	2.03	13	6.4	96.3
1305	P07951	TPM2_human	Tropomyosin beta chain (tropomyosin 2) (beta-tropomyosin)	1926	1238	0.001	1.6	-35.7	2.43	18	4.7	33.0
5610	Q9Y561	LRP12_human	Low-density lipoprotein receptor-related protein 12 (SR7)	190	264	0.001	1.4	38.8	2.41	11	7.4	64.0
7514	P50991	TCFD_human	T-complex protein 1, delta subunit	735	522	0.001	1.4	-29.1	2.43	21	7.7	58.3
1609	P05747	K2C3_human	Keratin 8, type II	1614	820	0.001	2.0	-49.2	2.43	18	5.5	53.5
2304	P07910	HNRPC_human	Heterogeneous nuclear ribonucleoprotein C, isoform a	627	292	0.001	2.1	-53.5	1.76	10	5.1	33.3
5603	P13647	K2C5_human	Keratin 5, type II	751	434	0.002	1.7	-42.2	1.87	17	7.7	62.6
1211	O60393	O60393_human	Craniofacial development protein 1; CP27 (Buxentau)	317	225	0.003	1.4	-29.2	2.43	12	4.8	33.6
5104	P04792	HSPB1_human	Heat shock 27kD protein 1; hspB1	1497	1945	0.003	1.3	29.9	1.34	26	6.0	22.8
7306	Q9BP27	SINI_human	Stress-activated map kinase interacting protein 1	444	337	0.004	1.3	-24.1	2.43	6	8.7	55.4
4205	Q14320	XAP5_human	XAP-5 protein	1394	1089	0.004	1.3	-22.1	1.17	31	5.8	32.7
5403	Q79955	FLOT1_human	Flotillin	729	339	0.01	2.2	-53.5	2.43	22	7.1	47.5
3505	P13645	K1C1_human	Keratin 10, type I	253	357	0.01	1.4	41.2	2.43	16	5.1	59.7
3822	Q9Y6F6	Q9Y6F6_human	JAW1-related protein, isoform a; inositol 1,4,5-triphosphate-associated cGMP kinase substrate	305	367	0.01	1.2	20.5	2.26	3	5.4	97.5
6605	P13647	K2C5_human	Keratin 5, type II	3172	4113	0.01	1.3	29.7	2.43	18	7.7	62.6
2815	P35913	PDB6B_human	Phosphodiesterase 6B, cGMP-specific, rod, beta	215	168	0.01	1.3	-21.6	2.35	5	5.1	99.4
4201	P12429	ANXA3_human	Annexin A3 (charge variant)	698	545	0.01	1.3	-21.9	2.43	38	6.0	30.1
6511	Q15124	PGM5_human	Phosphoglucomutase 5	360	272	0.01	1.3	-24.4	1.56	23	6.8	56.1
5002	P02735	SAA_human	Serum amyloid A protein beta	722	598	0.01	1.2	-17.1	2.43	49	5.6	11.7
7701	Q96BP3	Q96BP3_human	Cyclophilin; peptidyl-prolyl cis-trans isomerase	803	942	0.01	1.2	22.4	2.43	12	6.7	74.0
6806	Q9BSG3	Q9BSG3_human	Rab6-interacting protein 2 isoform alpha	116	97	0.01	1.2	-16.1	2.03	37	6.2	108.9
3801	Q9Y4E8	UBP15_human	Ubiquitin specific protease 15	782	637	0.01	1.2	-18.6	2.43	12	5.0	104.2
6712	Q13620	CUL4B_human	Cullin homolog 4B	327	450	0.01	1.4	37.8	2.43	13	6.4	84.5
5509	P13647	K2C5_human	Keratin 5, type II	447	519	0.01	1.4	-28.7	1.35	10	7.7	62.6
4406	G00233	PSD9_human	26S proteasome non-ATPase regulatory subunit 9	541	901	0.02	1.7	66.5	2.43	12	5.3	45.4
4502	Q15850	Q15850_human	Ulf-1ret protein, protein-tyrosine kinase (clone lambda-ret-5)	451	681	0.02	1.5	50.9	2.43	12	5.7	54.2
1104	Q9NUP1	CNO_human	Cappuccino protein homolog	1673	1582	0.02	1.2	-17.4	2.43	22	4.9	25.7

^a SSP: protein spot number assigned by PDQuest.

^b Prob: result of paired Student's test.

^c Z-score: from ProFound™ Database Search.

^d % coverage: percentage of total protein sequenced represented by measured peptide masses.

^e pI and MW: calculated based on sequence via ExPASy proteomics tools.

